Implications for oxidative stress and astrocytes following 26S proteasomal depletion in mouse forebrain neurones•

Jamal Elkharaz [a], Aslihan Ugun-Klusek [b], Tim Constantin-Teodosiu [a], Karen Lawler [a], R John Mayer [a], Ellen Billett [b], James Lowe [c], Lynn Bedford [a,]

[a] School of Biomedical Sciences, University of Nottingham, Nottingham, UK
[b] School of Science and Technology, Nottingham Trent University, Nottingham, UK
[c] Division of Histopathology, School of Molecular Medical Sciences, University of Nottingham, UK

a r t i c l e   i n f o

a b s t r a c t

Neurodegenerative diseases are characterized by progressive degeneration of selective neurones in the nervous system, but the underlying mechanisms involved in neuroprotection and neurodegeneration remain unclear. Dysfunction of the ubiquitin proteasome system is one of the proposed hypotheses for the cause and progression of neuronal loss. We have performed quantitative two-dimensional fluorescence difference in-gel electrophoresis combined with peptide mass fingerprinting to reveal proteome changes associated with neurodegeneration following 26S proteasomal depletion in mouse forebrain neurones. Differentially expressed proteins were validated by Western blotting, biochemical assays and immunohistochemistry. Of significance was increased expression of the antioxidant enzyme peroxiredoxin 6 (PRDX6) in astrocytes, associated with oxidative stress. Interestingly, PRDX6 is a bifunctional enzyme with antioxidant peroxidase and phospholipase A_2 (PLA_2) activities. The PLA_2 activity of PRDX6 was also increased following 26S proteasomal depletion and may be involved in neuroprotective or neurodegenerative mechanisms. This is the first in vivo report of oxidative stress caused directly by neuronal proteasome dysfunction in the mammalian brain. The results contribute to understanding neuronal–glial interactions in disease pathogenesis, provide an in vivo link between prominent disease hypotheses and importantly, are of relevance to a heterogeneous spectrum of neurodegenerative diseases.

1. Introduction

Neurodegenerative diseases are characterized by the progressive degeneration of selective neurones of the nervous system. Abnormal protein aggregation, impaired protein degradation, mitochondrial dysfunction and oxidative stress are key hypotheses for cause and progression of major human neurodegenerative diseases, including Alzheimer's disease (AD) and Parkinson's disease (PD) [1–3]. Attention has also turned to the contribution of glial cells to neurodegeneration [4], but the underlying mechanisms involved in neuroprotection and neurodegeneration in the nervous system remain unclear.

The ubiquitin proteasome system (UPS) is the major intracellular pathway for regulated degradation of unwanted proteins and central to normal cellular homeostasis [5]. A sequence of enzymes covalently attach polyubiquitin chains to unwanted proteins as a signal for degradation by the 26S proteasome. Studies in human brain and disease models have implicated dysfunction of the UPS in the pathological changes that lead to neurodegeneration [6–9]. Ubiquitin-positive protein inclusions are a common feature of human neurodegenerative diseases [6]. Also, in PD and dementia with Lewy bodies (DLB) patients, altered proteasome activity and subunit expression has been reported [7]. In a significant study, we showed that genetic depletion of 26S proteasomes in mouse brain neurones caused neurodegeneration and the formation of protein inclusions resembling human pale bodies, the precursor of Lewy bodies, providing a compelling link between UPS-mediated protein degradation and neurodegeneration [10].

Proteomic studies are of considerable interest to identify much-needed novel pathogenic mechanisms connected to neurodegenerative disease. There are inherent difficulties with a study of a mixture of cell-types in the brain, but it is essential to investigate in vivo models to identify the importance of neuronal–glial cellular interactions during disease development that are not revealed in studies of cell lines composed of a single clonal cell-type. We have employed a quantitative two-dimensional fluorescence difference in-gel electrophoresis (2D-DIGE) proteomic approach to reveal proteome changes associated with cortical neurodegeneration following 26S proteasomal depletion in our unique mouse model.

Corresponding author at: D37b School of Biomedical Sciences, University of Nottingham, Queens Medical Centre, Nottingham, NG2 7UH, UK. Tel.: + 44 1158230512.
E-mail address: lynn.bedford@nottingham.ac.uk (L. Bedford).

Protein changes identified in our 2D-DIGE study were validated by alternative approaches, namely 1D and 2D Western blotting as well as biochemical and immunohistochemical investigations to further understand their significance. The results show new information linking UPS dysfunction to oxidative stress in the brain in vivo and the importance of understanding neuronal–glial interactions during disease progression.

2. Materials and methods

2.1. 26S proteasomal depletion mouse model

Neurone-specific 26S proteasome-depleted mice were recreated using Cre/loxP conditional gene targeting as described in detail previously [10]. For forebrain, including cortex, neurone-specific inactivation of Psmc1, Cre recombinase was expressed under the control of the calcium calmodulin-dependent protein kinase IIα promoter (Psmc1$^{fl/fl}$; CaMKIIα-Cre) [10]. CaMKIIα is expressed in post-mitotic neurones from approximately post-natal week 2 [11,12]. Appropriate littermate mice were used as controls.

All procedures were carried out under personal and project licenses granted by the UK Home Office in accordance with the Animals (Scientific Procedures) Act 1986 and with ethical approval from the University of Nottingham Ethical Review Committee.

2.2. 2D fluorescence difference in-gel electrophoresis (2D-DIGE)

Mouse cortex was homogenized in lysis buffer containing 30 mM Tris–HCl pH 8.8, 8 M Urea and 4% (w/v) CHAPS, followed by centrifugation at 20,000 g for 5 min at 4 °C and collection of supernatant. Protein estimation used the Bio-Rad (Bradford) protein assay kit. CyDye labeling was performed according to the manufacturer's instructions (GE Healthcare) and incorporating a dye swap. 15 μg of each sample was labeled with Cy3 and Cy5, and a pooled sample was labeled with Cy2 containing equal amounts of all samples as an internal standard. 10 mM lysine was used to stop labeling. First dimension isoelectric focusing (IEF) used a Bio-Rad Protein IEF Cell and 7 cm 3–10 non-linear pH gradient IPG strips (Bio-Rad). Strips were passively rehydrated for 1 h, actively rehydrated for 13 h and 40 min at 50 V followed by IEF (250 V for 20 min linear, 4000 V for 2 h linear, 4000 V for 10,000 V/h rapid). The strips were incubated in 2% (w/v) dithiothreitol in equilibration buffer [50 mM Tris–HCl pH 8.8, 6 M Urea, 2% (w/v) sodium dodecyl sulfate (SDS) and 20% (v/v) glycerol] and then 2.5% (w/v) iodoacetamide in equilibration buffer for 15 min each. Strips were placed on top of 12–18% gradient SDS-PAGE resolving gels for the second dimension. A Fujifilm FLA-5100 scanner was used to scan each gel at the corresponding wavelengths to the CyDyes. Images were analyzed using SameSpots software (Progenesis) with a 1.2-fold change set as the cut off value and ANOVA (P b 0.05).

2.3. Mass spectrometry analysis

For identification of protein spots, gels were either silver (GE Healthcare) or Coomassie blue (Cheshire Sciences) stained using a mass spectrometry-compatible protocol. Spots were excised from the gel manually and washed three times with 50 μL of acetonitrile (ACN)/25 mM NH$_4$HCO$_3$ (2:1) for 15 min each followed by 50 μL of 25 mM NH$_4$HCO$_3$ for 10 min. Gel pieces were then air dried for 15 min and rehydrated in 5 μL of 12.5 ng/μL sequencing grade trypsin (Promega) on ice for 20 min. 5 μl of 25 mM NH$_4$HCO$_3$ was added to each tube and incubated at 37 °C for 4 h. Tryptic digests were collected, dried in a vacuum concentrator (Eppendorf) and 2 μl of 50% (v/v) ACN/0.1% (v/v) trifluoroacetic acid (TFA) was added to each tube. Finally, 0.5 μL of sample was transferred to the MALDI plate followed by 0.5 μL of 10 mg (w/v) α-cyano-4-hydroxycinnamic acid matrix (LaserBio Laboratories) in 50% (v/v) ACN/0.1% (v/v) TFA. Peptide mass fingerprints were generated using a MALDI-TOF mass spectrometer (Bruker Daltonics Ultraflex III MALDI-TOFTOF). Proteins were identified using the Mascot search engine (http://www.matrixscience.com); stating "Mus musculus" species, carbamidomethyl fixed and oxidized methionine as variable modifications and 100 ppm peptide tolerance. Positive identity was given by scores over 56 (comparing Swiss-Prot database) and their molecular mass and pI were compared to the position of the spot on the 2D gel.

2.4. Western blot analysis

Mouse cortex was homogenized as described in 2D-DIGE. 50–100 μg was mixed with 2× reducing sample buffer [150 mM Tris–HCl pH 6.8, 8 M Urea, 10% (v/v) SDS, 20% (v/v) glycerol, 10% (v/v) mercaptoethanol, 3% (w/v) dithiothreitol, 0.1% (w/v) bromophenol blue]. Proteins were separated using 12% SDS-PAGE and transferred to nitrocellulose membrane. Blocking was for 1 h in 5% (w/v) Marvel in Tris-buffered saline containing 0.1% (v/v) Tween 20. Incubation in primary and corresponding horseradish peroxidase-conjugated secondary antibodies (Sigma) was overnight at 4 °C and for 1 h at room temperature respectively in blocking solution. The primary antibodies used were: 1:1000 vimentin (GeneTex), peroxiredoxin 6 (GeneTex), glucose-regulated protein (Cell Signaling), protein disulphide isomerase (GeneTex), CCAAT-enhancer-binding protein homologous protein (Cell Signaling) and glial fibrillary acidic protein (Sigma); 1:500 fumerate hydratase (GeneTex); 1:250 stathmin (GeneTex); 1:200 X-box binding protein (Santa Cruz). Proteins were detected using enhanced chemiluminescence (Pierce). The band intensity was calculated with Quantity One 1-D analysis Software and/or Aida. For 2D Western blot analysis, samples were separated as described in 2D-DIGE and following the second dimension processed to Western blotting as described here.

2.5. Reactive oxygen species assay

Levels of reactive oxygen species were examined using the 2′,7′-dichlorofluorescein diacetate — cellular reactive oxygen species detection assay kit (abcam) according to the manufacturer's instructions. Detection used fluorescent spectroscopy with excitation and emission of 485 nm and 520 nm respectively.

2.6. Lipid peroxidation

Malondialdehyde (MDA) concentration was determined as an indicator of lipid peroxidation products based on the method of Erdelmeier et al. [13]. Mouse cortex was homogenized in 5 mM butylated hydroxytoluene in 20 mM phosphate buffer pH 7.4, followed by centrifugation at 3000 g for 10 min at 4 °C. Protein estimation used the Bio-Rad (Bradford) protein assay kit. 300 μl (9.5 μg/μl) was hydrolyzed using HCl pH 1–2 and incubated at 60 °C for 80 min. 60 μl of sample was mixed with 195 μl of 10.3 mM N-methyl-2-phenylindol in 3:1 (v/v) acetonitrile:methanol and then 45 μl of concentrated HCl, incubated at 45 °C for 60 min and centrifuged at 15,000 g for 10 min to clarify. Absorbance was measured spectrophotometrically at 586 nm. Concentration of malondialdehyde (μM/mg protein) was calculated using 1,1,3,3-tetramethoxypropane as a standard.

2.7. Phospholipase A$_2$ assay

Phospholipase A$_2$ (PLA$_2$) activity (U/ml/mg protein) was determined using EnzChek Phospholipase A2 Assay kit (Invitrogen) according to the manufacturer's instructions. Detection used fluorescent spectroscopy with excitation and emission of 485 nm and 520 nm respectively. MJ33 inhibitor was used at 3 mol% based on previous reports [14,15].

2.8. Protein oxidation

Protein carbonyl content (nM/mg protein) was determined utilizing the 2,4-dinitrophenylhydrazine (DNPH) reaction following Cayman's Protein Carbonyl Colorimetric Assay Kit according to the manufacturer's instructions. Absorbance was measured spectrophotometrically at 375 nm.

2.9. Immunohistochemistry

Mice were perfusion-fixed with 0.9% saline followed by 4% paraformaldehyde in phosphate buffered saline pH 7.4. The brains were then processed to paraffin with chloroform as the clearing agent. Immunohistochemistry was performed as directed in Vector Laboratories M.O.M Immunodetection [GFAP (Sigma)] or Vectastain Elite Rabbit IgG [PRDX6 (GeneTex) and MAP2 (abcam)] ABC kits using 0.01 M citrate buffer containing 0.05% Tween-20 pH 6 for antigen retrieval and appropriate fluorescently-conjugated secondary antibodies.

2.10. Statistical analysis

Results are expressed as mean average ± SEM. Statistical differences were analyzed by ANOVA and Student's t-test with significance set as indicated.

3. Results

3.1. 26S proteasomal depletion mouse model of neurodegeneration

Generation of neurone-specific 26S proteasome-depleted mice has been described in detail previously [10]. To summarize, the Cre/loxP system spatially restricts inactivation of an essential subunit of the 19S regulatory particle of the 26S proteasome, ATPase Psmc1. PSMC1 is necessary for the assembly and activity of the 26S proteasome [10]. For forebrain neurone-specific inactivation of Psmc1, including cortex, floxed Psmc1 mice were crossed with mice expressing Cre recombinase under the control of the calcium calmodulin-dependent protein kinase IIα promoter (Psmc1$^{fl/fl}$; CaMKIIα-Cre). CaMKIIα is expressed in post-mitotic neurones from approximately post-natal week 2. We previously showed that 26S proteasomal depletion in mouse cortical brain neurones caused neurodegeneration and the formation of intraneuronal inclusion bodies accompanied by reactive gliosis at 6 weeks of age [10]. The study here investigates proteomic changes accompanying neurodegeneration in the mouse cortex.

3.2. Differentially-expressed proteins in 26S proteasome-depleted cortex

Cortices from individual 6 week-old 26S proteasome-depleted and control (n = 4) mice were compared using 2D-DIGE proteomic analysis and Progenesis SameSpots to identify differentially-expressed proteins. Fig. 1 shows a representative 2D gel image. The expression level of 24 spots showed statistically significant changes between 26S proteasome-depleted and control animals (1.2-fold, ANOVA p b 0.05). Supplementary Table 1 lists the 19 proteins that were identified by peptide mass fingerprinting. The 2D-DIGE results and protein identifications were validated by Western blot analysis of selected differentially-expressed proteins based on antibody availability. We confirmed by 1D Western blotting that expression of glial fibrillary acidic protein (GFAP; Fig. 1, spot 2), vimentin (VIME; Fig. 1, spot 1) and peroxiredoxin 6 (PRDX6; Fig. 1, spot 10) was significantly increased while mitochondrial fumarate hydratase (FUMH; Fig. 1, spot 4) and stathmin (STMN1; Fig. 1, spot 11) were significantly decreased in 26S proteasome-depleted vs. control cortex consistent with the 2D-DIGE analysis (Fig. 2). GFAP and VIME are associated with the intermediate filament system in astrocytes and their up-regulation is a hallmark of astrocyte activation and the resulting
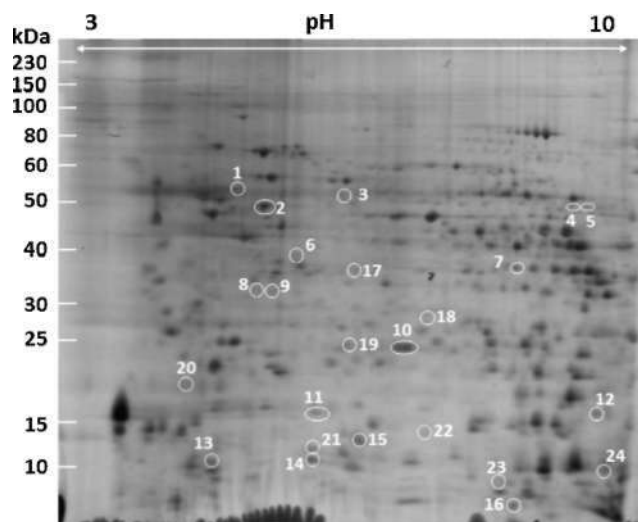

Fig. 1. Representative 2D gel image of mouse brain cortex homogenate labeled with Cy5 dye and differentially-expressed protein spots between 26S proteasome-depleted and control mouse cortices highlighted (spots 1–24). Numbered spots showed 1.2-fold change with statistical significance (ANOVA p b 0.05). Spots 1–16 were identified by peptide mass fingerprinting (Supplementary Table 1).

reactive gliosis [16]. This confirms our previously reported reactive astrogliosis by GFAP immunostaining of cortical brain sections following neuronal 26S proteasomal depletion [10]. PRDX6 has a well-known role as an antioxidant enzyme and its up-regulation in the cortex following 26S proteasomal depletion is suggestive of oxidative stress [17–22]. FUMH is a key enzyme of the tricarboxylic acid (TCA) cycle and STMN1 has an important function in microtubule dynamics [23].

2D gel electrophoresis can separate isoforms of the same protein, whereas 1D Western blotting provides a single band of total protein. Fig. 3 shows differential expression of GFAP isoforms in 6 week-old mice using 2D Western blot analysis. Two predominant isoforms of GFAP were detected in the control and 26S proteasome-depleted mouse cortices (Fig. 3; spots 1 and 2). Four additional GFAP isoforms were detected in the 26S proteasome-depleted cortex (Fig. 3; spots 3–6). Interestingly, GFAP was also identified in 2D-DIGE spot 9 (Fig. 1 and Supplementary Table 1) that may correspond to spot 5 or 6 in Fig. 3. We cannot exclude that the novel isoforms of GFAP detected in the 26S proteasome-depleted cortex may be present in the control cortex, but below the level of detection by this approach. GFAP isoforms may be associated with astrocyte subtypes that have specific functions and neuropathological conditions in the brain [24,25]. Alternatively, spots 5 and 6 may be GFAP protein breakdown products [26].

3.3. Neuronal 26S proteasomal depletion causes oxidative stress

Since oxidative stress is a pivotal factor in neuronal death in neurodegenerative diseases, we further investigated the antioxidant enzyme PRDX6 and oxidative stress in the mouse cortex following 26S proteasomal depletion.

To investigate the levels of reactive oxygen species (ROS) in 26S proteasome-depleted and control mouse cortices we used 2 ,7 -dichlorofluorescein diacetate fluorogenic dye. This is the most widely used assay for measuring oxidative stress [27]. The levels of ROS were significantly increased in 26S proteasome-depleted cortices at 2 and half weeks of age (t-test p b 0.05; Fig. 4A). Because CaMKIIα is expressed in cortical neurones from approximately postnatal week 2, the data indicate that the ensuing loss of PSMC1 and 26S proteasome activity causes oxidative stress. There was no significant difference in ROS levels between 26S proteasome-depleted and control mouse cortices at 3 weeks-old (Fig. 4B). At 4 and 6 weeks

A

Control   *Psmc1*^{fl/fl}*;CaMKIIα-Cre*

B   **C**

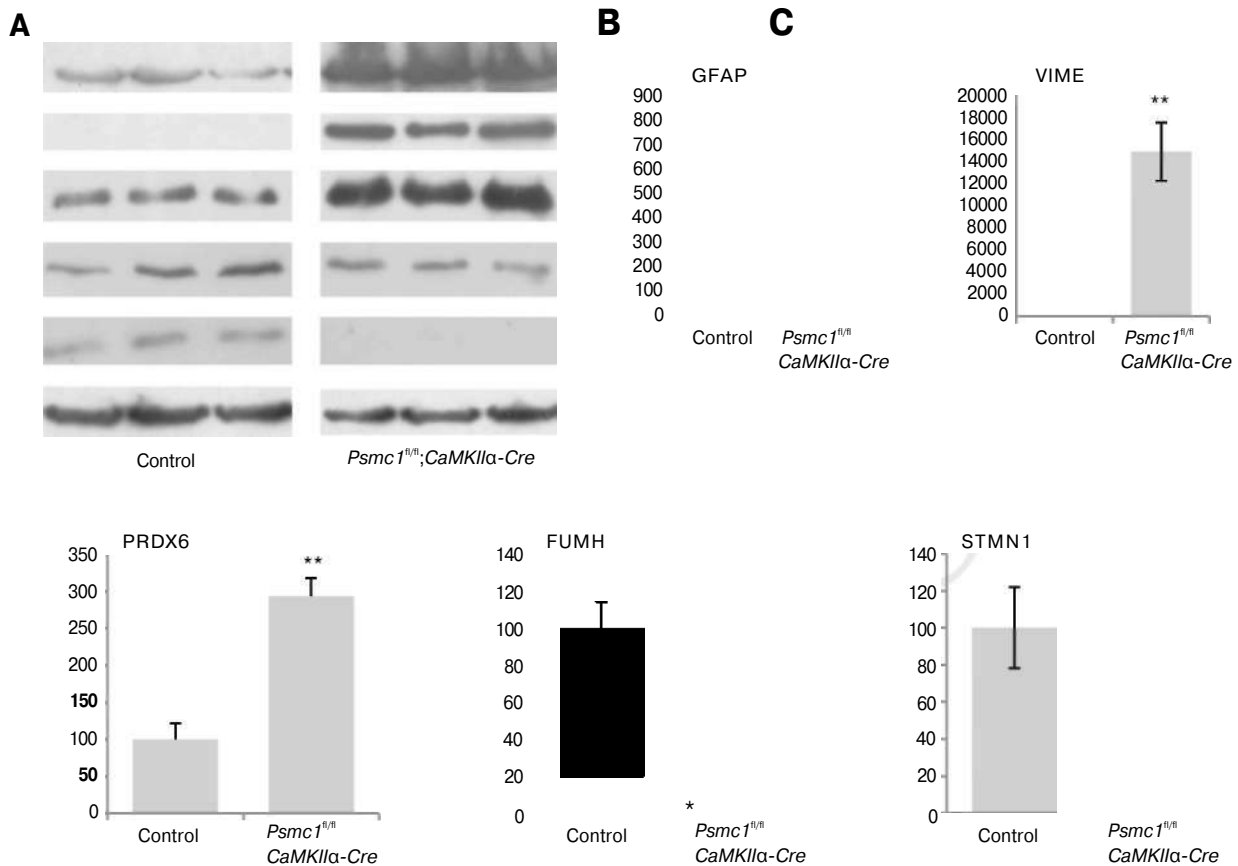GFAP

VIME

PRDX6   FUMH   STMN1

Fig. 2. Validation and quantitation of identified protein changes following 26S proteasomal depletion in mouse cortex. 1D Western blot analysis of total cortical homogenates from 6 week-old control and 26S proteasome-depleted (Psmc1$^{fl/fl}$; CaMKIIα-Cre) mice for GFAP, VIME, PRDX6, FUMH and STMN1. A representative β-actin loading control is shown; this was performed for each Western blot. (B–F) Densitometry used QuantityOne software. Values were normalized to β-actin and represented as % vs. controls. Error bars represent SEM. n 3, *p b 0.05, **p b 0.01 (Student's t-test).

of age there was a significant decrease in the levels of ROS in 26S proteasome-depleted cortices compared to controls (t-test p b 0.01; Fig. 4C and D). Linear regression analysis showed a significant correlation between age and the levels of ROS in 26S proteasome-depleted cortex (p b 0.05; Fig. 4E). There was also a significant correlation between age and the levels of PRDX6 protein expression in 26S proteasome-depleted cortex between 2 and 6 weeks-old (p b 0.01; Fig. 4E). Importantly, there was an inverse relationship between the levels of PRDX6 protein expression and ROS in 26S proteasome-depleted mouse cortex with increasing age, indicative of an antioxidant response of PRDX6 (Fig. 4E).

3.4. Neuronal 26S proteasomal depletion causes increased lipid peroxidation

High polyunsaturated fatty acid content makes the brain particularly susceptible to oxidative stress-associated lipid damage. Also, lipid peroxidation is known to be an autocatalytic process, amplifying the destructive effects of the initial free radical [28,29]. Quantitation
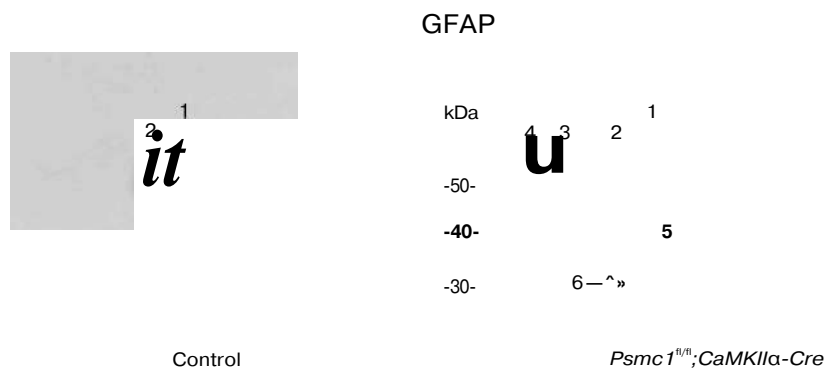
GFAP

Control   *Psmc1*^{fl/fl}*;CaMKIIα-Cre*

Fig. 3. Protein isoform expression of GFAP revealed by 2D Western blotting of control and 26S proteasome-depleted (Psmc1$^{fl/fl}$; CaMKIIα-Cre) mouse cortices. Arrows indicate six GFAP isoforms.
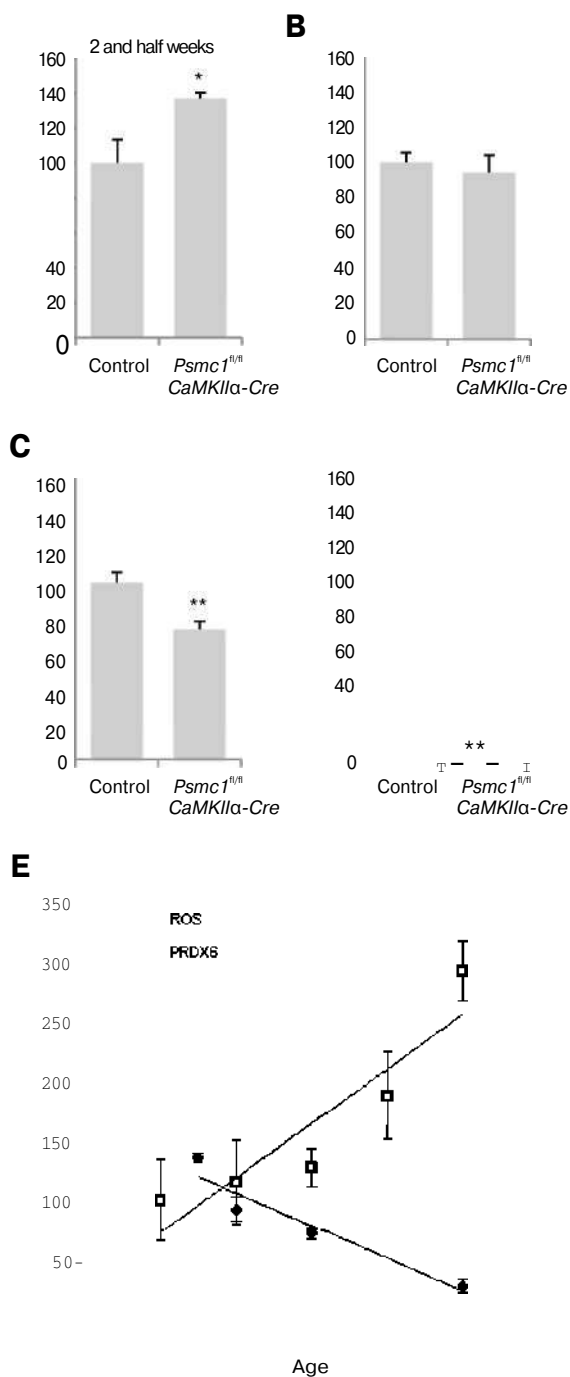
Fig. 4. Increased PRDX6 protein expression is associated with decreased reactive oxygen species (ROS). Levels of ROS (A–D) in control and 26S proteasome-depleted (Psmc1^{fl/fl}; CaMKIIα-Cre) cortices. Data represented as mean ± SEM. n ≥ 6, *p b 0.05, **p b 0.01 (Student's t-test). (E) Inverse relationship between the levels of PRDX6 protein expression and ROS in 26S proteasome-depleted mouse cortex with increasing age. Data represented as mean ± SEM.

of malondialdehyde (MDA), a toxic secondary product of membrane lipid peroxidation, in cortical tissue homogenates between 4 and 6 weeks of age identified significantly increased levels of MDA in 5 and 6 week-old 26S proteasome-depleted mice compared to controls (t-test p b 0.01; Fig. 5A–C), indicating that lipid oxidation is increased following neuronal 26S proteasomal depletion.

Protein carbonyls are hallmarks of the oxidative status of proteins. Therefore, to further investigate oxidative stress, we evaluated carbonyl content spectrophotometrically using a reaction with 2,4-dinitrophenylhydrazine in mouse cortical tissue homogenates.

No significant difference in the levels of protein carbonyls was observed between 26S proteasome-depleted and control mouse cortices at 6 weeks-old (Supplementary Fig. 1).

3.5. Increased phospholipase A_2 activity in 26S proteasome-depleted cortex

Interestingly, PRDX6 is a bifunctional enzyme with peroxidase and phospholipase A_2 (PLA_2) activities [30]. The PLA_2 activity of PRDX6 has not been studied as widely as the peroxidase-associated antioxidant properties. Quantitation of PLA_2 activity in 26S proteasome-depleted and control cortical homogenates between 4 and 6 weeks of age showed significantly increased activity in the 6 week-old 26S proteasome-depleted mouse cortex (t-test p b 0.01; Fig. 5D–F). The chemical inhibitor MJ33 that has previously been shown to have some (although not total) specificity for PRDX6 PLA_2 activity [14,15] significantly decreased PLA_2 activity in 26S proteasome-depleted cortex, suggesting that some of the PLA_2 activity was associated with PRDX6 (Fig. 5F).

3.6. Astrocytic localization of PRDX6

To investigate the cellular localization of PRDX6 we performed double immunofluorescent labeling of brain sections with PRDX6 and GFAP or 200 kD neurofilament heavy chain (NF-H) for astrocytes and neurones respectively (Fig. 6 and Supplementary Fig. 2). PRDX6 immunolabeled cells with the characteristic morphology of astrocytes in control and 26S proteasome-depleted cortices from 6 week-old mice (Fig. 6). Double-labeling with GFAP confirmed the localization of PRDX6 in astrocytes in the 26S proteasome-depleted mice (Fig. 6; right-hand panel). GFAP is the most widely used marker for immunohistochemical identification of astrocytes and labels reactive astrocytes that are responding to central nervous system (CNS) damage, but it is recognized that not all non-reactive astrocytes in the healthy CNS are identified by GFAP [31]. Therefore, PRDX6 expression in the control mouse brain is in non-reactive astrocytes that are not immunohistochemically labeled by GFAP (Fig. 6; left-hand panel). Importantly, we noted a much higher diffuse PRDX6 staining in the 26S proteasome-depleted cortical brain sections compared to the control (Fig. 6; compare i and ii), suggesting PRDX6 may be secreted by activated astrocytes in response to the neuronal changes. The expression of PRDX6 did not co-localize with NF-H in mouse cortical neurones (Supplementary Fig. 2).

4. Discussion

Proteomic studies of human post-mortem brain and disease models are of considerable interest to understand pathogenic mechanisms connected to neurodegenerative disease. This study has identified and validated several differentially-expressed proteins accompanying neurodegeneration in the mouse cortex following neuronal 26S proteasomal depletion. Among these, the antioxidant enzyme PRDX6 was significantly increased. Since oxidative stress is a pivotal factor in human neurodegenerative diseases [32,33], supported by animal and cellular models [33–35], we further investigated PRDX6 and oxidative stress in the 26S proteasome-depleted mouse cortex.

Here we have shown a significant inverse relationship between the levels of PRDX6 protein expression and ROS following 26S proteasomal depletion in the mouse cortical neurones, indicative of oxidative stress and an antioxidant response of PRDX6. Lipid peroxidation was also significantly increased in the cortex of 26S proteasome-depleted mice. Similar to the other PRDXs and glutathione peroxidase family, PRDX6 can reduce hydrogen peroxide and short chain hydroperoxides, but PRDX6 can also directly bind and reduce phospholipid hydroperoxides [36,37]. This characteristic plays an important role in its antioxidant defense [19,20]. Studies in cell and mouse models demonstrate that
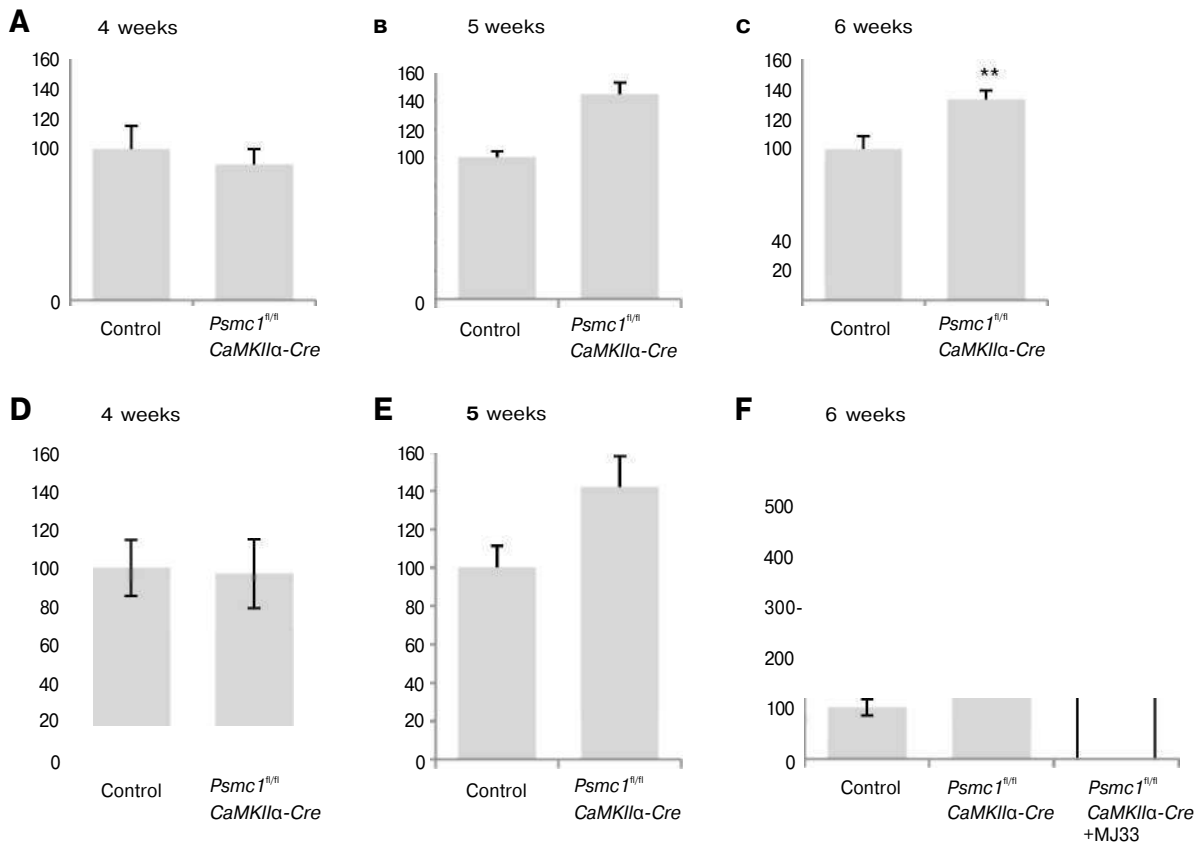
Fig. 5. Neuronal 26S proteasomal depletion causes increased lipid peroxidation and PRDX6 PLA$_2$ activity. Quantitation of MDA (A–C) and PLA$_2$ activity (D–F) in control and 26S proteasome-depleted (Psmc1$^{fl/fl}$; CaMKIIα-Cre) cortices at 4, 5 and 6 weeks of age. (F) PLA$_2$ activity is significantly decreased by chemical inhibitor MJ33 at 6 weeks of age. Data presented as mean ± SEM. n   4, **p b 0.01 (Student's t-test).

decreased expression or overexpression of PRDX6 results in increased sensitivity or resistance to oxidant stress respectively [17–22].

PRDX6 is a bifunctional enzyme with peroxidase and PLA$_2$ activities [30]. Increased PLA$_2$ activity in 26S proteasome-depleted cortex correlates with increased PRDX6 expression. Given previous studies have shown that the PLA$_2$ activity of PRDX6 is sensitive to MJ33 [14,15], we propose that the decreased PLA$_2$ activity in the presence of MJ33 is partly attributable to PRDX6. However, we recognize that MJ33 is not totally specific for PRDX6 and that other phospholipases that have not been investigated in this study presumably explain the MJ33-insensitive PLA$_2$ activity [38].

The PLA$_2$ activity of PRDX6 has been associated with several cellular functions. PLA$_2$ enzyme activity liberates both a free fatty acid and lysophosphatidylcholine from phosphatidylcholine substrates and has been implicated in oxidative stress-induced apoptosis and inflammation [39–42]. Importantly, a recent study in pulmonary microvascular endothelial cells suggested that the PLA$_2$ activity of PRDX6 may also play a role in antioxidant protection provided by PRDX6 [43].

The cellular distribution of PRDX6 in our mouse model is similar to previous studies in mouse and human brain showing expression of PRDX6 mainly in astrocytes [44–49]. A study in mouse brain neural cell types showed differential expression patterns of the six mammalian isoforms of the PRDX family and only PRDX6 was found in astrocytes, which may be indicative of a specific role in their function [46]. Importantly, an increase in PRDX6 and the number and staining intensity of PRDX6-positive astrocytes has been described in human brain regions affected in AD, PD and DLB, as well as other neurodegenerative disease mouse models [44,45,47,49,50]. Since oxidative stress is regarded as a fundamental process in the events that lead to neurodegeneration, the antioxidant function of PRDX6 may play an important neuroprotective response of the astrocyte [32,51,52]. Further support for PRDX6 in this

context was shown in parkin-deficient mice, where PRDX6 was downregulated [53].

We also noted a much higher diffuse PRDX6 staining in the 26S proteasome-depleted cortical brain sections compared to the control, suggesting PRDX6 may be secreted by activated astrocytes. This is supported by previous studies that have suggested that this enzyme may be a secreted protein [44,54]. Evidence suggests PRDX6 is present at very low levels in neurones and an early study in PD and DLB disease brains demonstrated the presence of PRDX6 in Lewy bodies [44,46–49]. However, PRDX6 expression was not detectable in neurones or inclusion bodies in our mouse model.

This is the first in vivo report of oxidative stress caused directly by neuronal 26S proteasome dysfunction in the mammalian brain. Our findings are supported by cellular studies using chemical proteasome inhibitors [55–57]. Various antioxidant defenses have also been demonstrated in response to proteasome inhibitor oxidative stress [57], but PRDX6 has not been described previously and most likely because studies were not focused on the brain. Since the high polyunsaturated fatty acid content makes the brain particularly susceptible to lipid peroxidation, the unique ability of PRDX6 to reduce phospholipid hydroperoxides may play an important role in antioxidant protection in the brain.

Increased astrocytic PRDX6 expression was associated with decreased levels of ROS, and together with the presence of oxidative stress, supports an antioxidant neuroprotective role of astrogliosis in response to neurodegeneration caused by 26S proteasome depletion in mouse brain neurones. However, the astrocytic network has a wide range of activities that can be both beneficial and detrimental such as energy metabolism and the release of inflammatory molecules respectively [31,58]. We emphasize that the PLA$_2$ activity of PRDX6 may also be involved in the production of further mediators

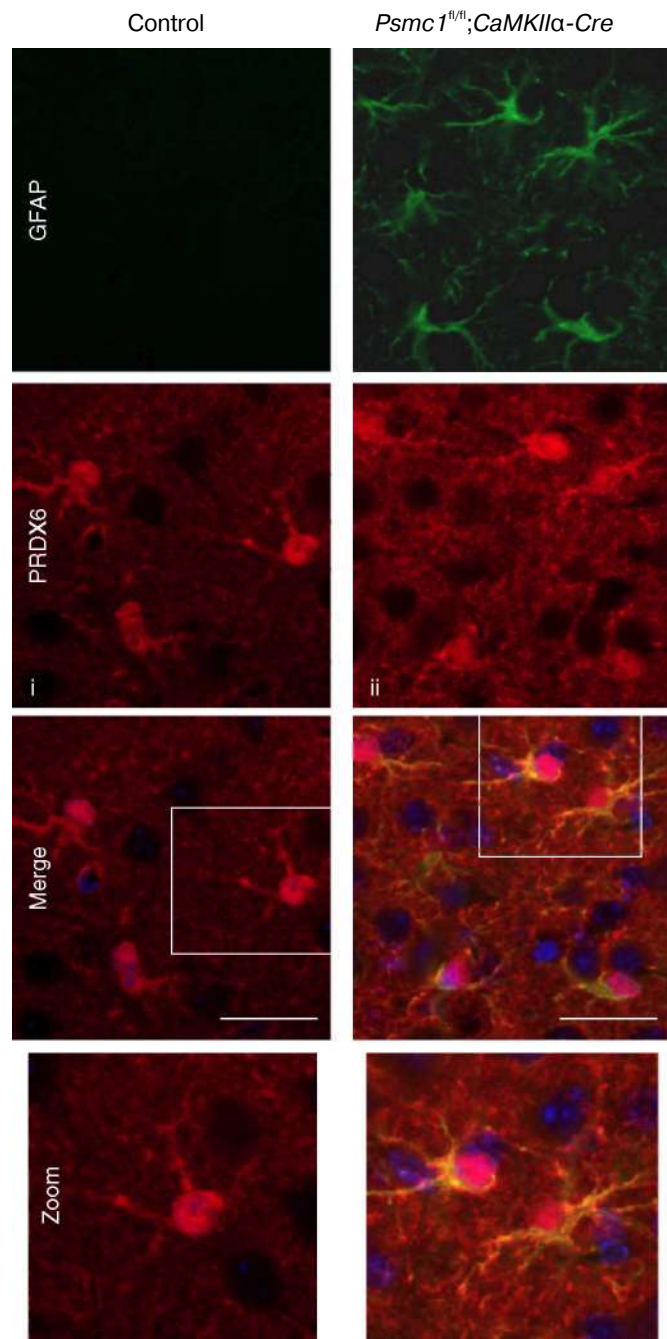Control $Psmc1^{fl/fl}$;CaMKIIα-Cre

Fig. 6. Astrocytic localization of PRDX6 in the mouse cortex. Double immunofluorescent labeling of cortical brain sections from control and 26S proteasome-depleted (Psmc1$^{fl/fl}$; CaMKIIα-Cre) 6 week-old mice with GFAP (green) and PRDX6 (red). DAPI (blue) was used as a fluorescent nuclear counterstain. Enlarged views of the boxed areas are shown (zoom). Note much higher diffuse PRDX6 staining in the 26S proteasome-depleted cortical brain sections in addition to the more focused staining in astrocytes (compare i and ii). Scale bar, 50 μm.

437 related to cellular signaling functions that may be protective or dele-
438 terious in the progressive neuronal loss.
439   The intercellular signaling molecule(s) and mechanism(s) that
440 modulate reactive astrogliosis in response to neurodegeneration fol-
441 lowing 26S proteasomal depletion in neurones will require further
442 study. Diverse molecules have been suggested that can be released
443 by all central nervous system cell-types, including ROS [58,59]. In-
444 terestingly, we report here that mitochondrial FUMH, a key enzyme
445 of the TCA cycle, is decreased in the 26S proteasome-depleted cortex

and may reflect mitochondrial dysfunction. We recently reported 446 that 26S proteasomal depletion in mouse brain neurones leads to the 447 formation of inclusions composed predominantly of morphologically 448 abnormal mitochondria with disrupted or disintegrated cristae [60]. A 449 spectrum of mitochondrial pathologies that may be associated with 450 oxidative stress has been described in human neurodegenerative 451 diseases and associated disease models, including perturbed respiratory 452 chain function, mitochondrial dynamics and clearance [32,33,61]. 453 Therefore, we suggest that mitochondrial dysfunction may be impor- 454 tant in the mechanism of oxidative stress and neurodegeneration 455 following 26S proteasome depletion. 456

Proteasome inhibition is known to induce endoplasmic reticulum 457 (ER) stress and activation of the unfolded protein response (UPR) 458 signaling pathways [62–64]. ER stress is associated with the production 459 of ROS from the ER as well as mitochondria and evidence of ER stress 460 has been shown in various human neurodegenerative diseases, such 461 as AD and PD [65–68]. Investigation of key mammalian ER 462 stress-induced proteins; the chaperone glucose-regulated protein 78 463 (GRP78), the transcription factor X-box binding protein-1 (XBP1), 464 protein disulphide isomerase (PDI) and the cell death mediator 465 CCAAT-enhancer-bindingprotein homologous protein (CHOP), showed 466 that neuronal 26S proteasomal depletion does not cause activation of 467 the UPR (Supplementary Fig. 3) [69,70]. Taken together, ER stress is 468 not an important source of ROS in this model. 469

Although we found evidence for increased oxidation of lipids 470 indicative of oxidative stress in the cortex following neuronal 471 26S proteasome depletion, protein oxidation was not increased. 472 Proteasome function is known to be important for the degradation 473 of oxidatively modified proteins [71–75]. Therefore, we may have 474 expected to find increased protein oxidation following 26S 475 proteasome depletion in the mouse cortex due to increased oxida- 476 tive stress and/or decreased removal of oxidatively modified 477 proteins. However, in the heterogeneous population of cellular 478 proteasome complexes, the 26S proteasome has a relatively minor 479 role in the removal of oxidatively damaged proteins compared to 480 the 20S proteasome [72,73,76–78]. We previously showed that 481 inactivation of Psmc1 specifically disrupts 26S proteasome function; 482 assembly and activity of the 20S core proteolytic proteasome was 483 not affected [10]. Therefore, 20S proteasome function in Psmc1; 484 CaMKIIα-Cre neurones may be sufficient to protect cells from protein 485 oxidative modification. Alternatively, it is possible that the level of 486 protein oxidation was not sufficient for detection in a mixed cell 487 population of targeted (CaMKIIα) and non-targeted neurones and 488 glia. 489

Different quantitative proteomic approaches will favor different 490 subpopulations of proteins. 2D-DIGE fluorescence-based detection 491 provides high sensitivity that is linear over several orders of magni- 492 tude [79,80]. The significant advantage of this technology is the ability 493 to multiplex using different fluorescent cyanine dyes, providing 494 greater accuracy of quantitation over conventional 2D gel approaches 495 [79]. However, the percentage of lysine residues in proteins may 496 affect labeling efficiency and current in-gel digestion and mass spec- 497 trometers limit identification of lesser abundant proteins detected 498 by 2D-DIGE [79]. Together with the well-known limitations of 2D 499 gel electrophoresis, i.e. hydrophobic proteins, dynamic range and 500 quantitative distribution issues, our study may miss some important 501 molecular players involved in the orchestration of cellular events 502 following neuronal 26S proteasomal depletion [79–81]. 503

In conclusion, we reveal that oxidative stress may contribute 504 to the cellular events leading to neurodegeneration following UPS 505 dysfunction, providing a novel intersection between two prominent 506 hypotheses in disease pathogenesis. Increased astrocytic expression 507 of PRDX6 also reveals innovative information regarding the role of 508 neuronal–glial interactions and astrogliosis in neurodegeneration. 509

Supplementary data to this article can be found online at http:// 510 dx.doi.org/10.1016/j.bbadis.2013.07.002. 511

References

[1] A.H. Schapira, P. Jenner, Etiology and pathogenesis of Parkinson's disease, Mov. Disord. 26 (2011) 1049–1055.

[2] K. Leuner, W.E. Muller, A.S. Reichert, From mitochondrial dysfunction to amyloid beta formation: novel insights into the pathogenesis of Alzheimer's disease, Mol. Neurobiol. 46 (2012) 186–193.

[3] T. Morawe, C. Hiebel, A. Kern, C. Behl, Protein homeostasis, aging and Alzheimer's disease, Mol. Neurobiol. 46 (2012) 41–54.

[4] E. Croisier, M.B. Graeber, Glial degeneration and reactive gliosis in alpha-synucleinopathies: the emerging concept of primary gliodegeneration, Acta Neuropathol. 112 (2006) 517–530.

[5] A.L. Goldberg, Protein degradation and protection against misfolded or damaged proteins, Nature 426 (2003) 895–899.

J. Lowe, A. Blanchard, K. Morrell, G. Lennox, L. Reynolds, M. Billett, M. Landon, R.J. Mayer, Ubiquitin is a common factor in intermediate filament inclusion bodies of diverse type in man, including those of Parkinson's disease, Pick's disease, and Alzheimer's disease, as well as Rosenthal fibres in cerebellar astrocytomas, cytoplasmic bodies in muscle, and Mallory bodies in alcoholic liver disease, J. Pathol. 155 (1988) 9–15.

[7] D. Ebrahimi-Fakhari, L. Wahlster, P.J. McLean, Protein degradation pathways in Parkinson's disease: curse or blessing, Acta Neuropathol. 124 (2012) 153–172.

[8] F.J. Dennissen, N. Kholod, F.W. van Leeuwen, The ubiquitin proteasome system in neurodegenerative diseases: culprit, accomplice or victim? Prog. Neurobiol. 96 (2012) 190–207.

[9] M. Orre, W. Kamphuis, S. Dooves, L. Kooijman, E.T. Chan, C.J. Kirk, V. Dimayuga Smith, S. Koot, C. Mamber, A.H. Jansen, H. Ovaa, E.M. Hol, Reactive glia show increased immunoproteasome activity in Alzheimer's disease, Brain 136 (2013) 1415–1431.

[10] L. Bedford, D. Hay, A. Devoy, S. Paine, D.G. Powe, R. Seth, T. Gray, I. Topham, K. Fone, N. Rezvani, M. Mee, T. Soane, R. Layfield, P.W. Sheppard, T. Ebendal, D. Usoskin, J. Lowe, R.J. Mayer, Depletion of 26S proteasomes in mouse brain neurons causes neurodegeneration and Lewy-like inclusions resembling human pale bodies, J. Neurosci. 28 (2008) 8189–8198.

[11] M. Mayford, M.E. Bach, Y.Y. Huang, L. Wang, R.D. Hawkins, E.R. Kandel, Control of memory formation through regulated expression of a CaMKII transgene, Science 274 (1996) 1678–1683.

[12] J.Z. Tsien, D.F. Chen, D. Gerber, C. Tom, E.H. Mercer, D.J. Anderson, M. Mayford, E.R. Kandel, S. Tonegawa, Subregion- and cell type-restricted gene knockout in mouse brain, Cell 87 (1996) 1317–1326.

[13] I. Erdelmeier, D. Gerard-Monnier, J.C. Yadan, J. Chaudiere, Reactions of N-methyl-2-phenylindole with malondialdehyde and 4-hydroxyalkenals. Mechanistic aspects of the colorimetric assay of lipid peroxidation, Chem. Res. Toxicol. 11 (1998) 1184–1194.

[14] A.B. Fisher, C.Dodia, A. Chander,M. Jain, A competitive inhibitor of phospholipase A2 decreases surfactant phosphatidylcholine degradation by the rat lung, Biochem. J. 288 (Pt 2) (1992) 407–411.

[15] A.B. Fisher, C. Dodia, Role of phospholipase A2 enzymes in degradation of dipalmitoylphosphatidylcholine by granular pneumocytes, J. Lipid Res. 37 (1996) 1057–1064.

[16] M. Pekny, M. Nilsson, Astrocyte activation and reactive gliosis, Glia 50 (2005) 427–434.

[17] Y. Manevich, T. Sweitzer, J.H. Pak, S.I. Feinstein, V. Muzykantov, A.B. Fisher, 1-Cys peroxiredoxin overexpression protects cells against phospholipid peroxidation-mediated membrane damage, PNAS 99 (2002) 11599–11604.

[18] X. Wang, S.A. Phelan, K. Forsman-Semb, E.F. Taylor, C.Petros, A.Brown, C.P. Lerner, B. Paigen, Mice with targeted mutation of peroxiredoxin 6 develop normally but are susceptible to oxidative stress, J. Biol. Chem. 278 (2003) 25179–25190.

[19] Y. Wang, S.I. Feinstein, Y. Manevich, Y.S. Ho, A.B. Fisher, Lung injury and mortality with hyperoxia are increased in peroxiredoxin 6 gene-targeted mice, Free Radic. Biol. Med. 37 (2004) 1736–1743.

[20] Y. Wang, S.I. Feinstein, Y. Manevich, Y.S. Ho, A.B. Fisher, Peroxiredoxin 6 gene-targeted mice show increased lung injury with paraquat-induced oxidative stress, Antioxid. Redox Signal. 8 (2006) 229–237.

[21] Y. Wang, S.A. Phelan, Y. Manevich, S.I. Feinstein, A.B. Fisher, Transgenic mice overexpressing peroxiredoxin 6 show increased resistance to lung injury in hyperoxia, Am. J. Respir. Cell Mol. Biol. 34 (2006) 481–486.

[22] Y. Wang, S.I. Feinstein, A.B. Fisher, Peroxiredoxin 6 as an antioxidant enzyme: protection of lung alveolar epithelial type II cells from H_2O_2-induced oxidative stress, J. Cell. Biochem. 104 (2008) 1274–1285.

[23] L. Jourdain, P. Curmi, A. Sobel, D. Pantaloni, M.F. Carlier, Stathmin: a tubulin-sequestering protein which forms a ternary T2S complex with two tubulin molecules, Biochemistry 36 (1997) 10817–10821.

[24] J. Middeldorp, E.M. Hol, GFAP in health and disease, Prog. Neurobiol. 93 (2011) 421–443.

[25] W. Kamphuis,C. Mamber, M. Moeton, L. Kooijman, J.A. Sluijs, A.H. Jansen, M.Verveer, L.R. de Groot, V.D. Smith, S. Rangarajan, J.J. Rodriguez, M. Orre, E.M. Hol, GFAP isoforms in adult mouse brain with a focus on neurogenic astrocytes and reactive astrogliosis in mouse models of Alzheimer disease, PLoS One 7 (2012) e42823.

[26] J.S. Zoltewicz, D. Scharf, B. Yang, A. Chawla, K.J. Newsom, L. Fang, Characterization of antibodies that detect human GFAP after traumatic brain injury, Biomark. Insights 7 (2012) 71–79.

[27] B. Kalyanaraman, V. Darley-Usmar, K.J. Davies, P.A. Dennery, H.J. Forman, M.B. Grisham, G.E. Mann, K. Moore, LJ. Roberts II, H. Ischiropoulos, Measuring reactive oxygen and nitrogen species with fluorescent probes: challenges and limitations, Free Radic. Biol. Med. 52 (2012) 1–6.

[28] B.A. Freeman, J.D. Crapo, Biology of disease: free radicals and tissue injury, Lab. Invest. 47 (1982) 412–426.

[29] T.F. Slater, Free-radical mechanisms in tissue injury, Biochem. J. 222 (1984) 1–15.

[30] A.B. Fisher, Peroxiredoxin 6: a bifunctional enzyme with glutathione peroxidase and phospholipase A(2) activities, Antioxid. Redox Signal. 15 (2011) 831–844.

[31] M.V. Sofroniew, H.V. Vinters, Astrocytes: biology and pathology, Acta Neuropathol. 119 (2010) 7–35.

[32] S. Gandhi, A.Y. Abramov, Mechanism of oxidative stress in neurodegeneration, Oxid. Med. Cell. Longev. (2012), (428010).   Q3

[33] M. Varcin, E. Bentea, Y. Michotte, S. Sarre, Oxidative stress in genetic mouse models of Parkinson's disease, Oxid. Med. Cell. Longev. (2012), (624925).   Q4

[34] J.K. Andersen, Oxidative stress in neurodegeneration: cause or consequence? Nat. Med. 10 (2004) S18–25, (Suppl.).

[35] D. Pratico, Evidence of oxidative stress in Alzheimer's disease brain and antioxidant therapy: lights and shadows, Ann. N. Y. Acad. Sci. 1147 (2008) 70–78.

[36] A.B. Fisher, C. Dodia, Y. Manevich, J.W. Chen, S.I. Feinstein, Phospholipid hydro-peroxides are substrates for non-selenium glutathione peroxidase, J. Biol. Chem. 274 (1999) 21326–21334.

[37] Y. Manevich, T. Shuvaeva, C. Dodia, A. Kazi, S.I. Feinstein, A.B. Fisher, Binding of peroxiredoxin 6 to substrate determines differential phospholipid hydroperoxide peroxidase and phospholipase A(2) activities, Arch. Biochem. Biophys. 485 (2009) 139–149.

[38] M.K. Jain, B.Z. Yu, J. Rogers, G.N. Ranadive, O.G. Berg, Interfacial catalysisby phospho-lipase A2: dissociation constants for calcium, substrate, products, and competitive inhibitors, Biochemistry 30 (1991) 7306–7317.

[39] P.J. Leavey, C. Gonzalez-Aller, G. Thurman, M. Kleinberg, L. Rinckel, D.W. Ambruso, S. Freeman, F.A. Kuypers, D.R. Ambruso, A 29-kDa protein associated with p67phox expresses both peroxiredoxin and phospholipase A2 activity and enhances superoxide anion production by a cell-free system of NADPH oxidase activity, J. Biol. Chem. 277 (2002) 45181–45187.

[40] S. Chatterjee, S.I. Feinstein, C. Dodia, E. Sorokina, Y.C. Lien, S. Nguyen, K. Debolt, D. Speicher, A.B. Fisher, Peroxiredoxin 6 phosphorylation and subsequent phospholipase A2 activity are required for agonist-mediated activation of NADPH oxidase in mouse pulmonary microvascular endothelium and alveolar macrophages, J. Biol. Chem. 286 (2011) 11696–11706.

[41] S.Y. Kim, E. Chun, K.Y. Lee, Phospholipase A(2) of peroxiredoxin 6 has a critical role in tumor necrosis factor-induced apoptosis, Cell Death Differ. 18 (2011) 1573–1583.

[42] D.R. Ambruso, M.A. Ellison, G.W. Thurman, T.L. Leto, Peroxiredoxin 6 translocates to the plasma membrane during neutrophil activation and is required for optimal NADPH oxidase activity, Biochim. Biophys. Acta 1823 (2012) 306–315.

[43] Y.C. Lien, S.I. Feinstein, C. Dodia, A.B. Fisher, The roles of peroxidase and phospholipase A2 activities of peroxiredoxin 6 in protecting pulmonary microvascular endothelial cells against peroxidative stress, Antioxid. Redox Signal. 16 (2012) 440–451.

[44] J.H. Power, J.M. Shannon, P.C. Blumbergs, W.P. Gai, Nonselenium glutathione peroxidase in human brain: elevated levels in Parkinson's disease and dementia with Lewy bodies, Am. J. Pathol. 161 (2002) 885–894.

[45] C.W. Strey, D. Spellman, A. Stieber, J.O. Gonatas, X. Wang, J.D. Lambris, N.K. Gonatas, Dysregulation of stathmin, amicrotubule-destabilizing protein, and up-regulation of Hsp25, Hsp27, and the antioxidant peroxiredoxin 6 in a mouse model of familial amyotrophic lateral sclerosis, Am. J. Pathol. 165 (2004) 1701–1718.

[46] M.H. Jin, Y.H. Lee, J.M. Kim, H.N. Sun, E.Y. Moon, M.H. Shong, S.U. Kim, S.H. Lee, T.H. Lee, D.Y. Yu, D.S. Lee, Characterization of neural cell types expressing peroxiredoxins in mouse brain, Neurosci. Lett. 381 (2005) 252–257.

[47] J.H. Power, S. Asad, T.K. Chataway, F. Chegini, J. Manavis, J.A. Temlett, P.H. Jensen, P.C. Blumbergs, W.P. Gai, Peroxiredoxin 6 in human brain: molecular forms, cellular distribution and association with Alzheimer's disease pathology, Acta Neuropathol. 115 (2008) 611–622.

[48] J. Goemaere, B. Knoops, Peroxiredoxin distribution inthe mouse brain with emphasis on neuronal populations affected in neurodegenerative disorders, J. Comp. Neurol. 520 (2011) 258–280.

[49] K. Yata, S. Oikawa, R. Sasaki, A. Shindo, R. Yang, M. Murata, K. Kanamaru, H. Tomimoto, Astrocytic neuroprotection through induction of cytoprotective molecules; a proteomic analysis of mutant P301S tau-transgenic mouse, Brain Res. 1410 (2011) 12–23.

[50] K. Krapfenbauer, E. Engidawork, N. Cairns, M. Fountoulakis, G. Lubec, Aberrant expression of peroxiredoxin subtypes in neurodegenerative disorders, Brain Res. 967 (2003) 152–160.

[51] M.F. Beal, Oxidatively modified proteins in aging and disease, Free Radic. Biol. Med. 32 (2002) 797–803.

[52] C. Pimentel, L. Batista-Nascimento, C. Rodrigues-Pousada, R.A. Menezes, Oxidative stress in Alzheimer's and Parkinson's diseases: insights from the yeast Saccharomyces cerevisiae, Oxid. Med. Cell. Longev. 2012 (2012) 132146.

[53] J.J. Palacino, D. Sagi, M.S. Goldberg, S. Krauss, C. Motz, M. Wacker, J. Klose, J. Shen, Mitochondrial dysfunction and oxidative damage in parkin-deficient mice, J. Biol. Chem. 279 (2004) 18614–18622.

[54] X.Z. Zhang, Z.F. Xiao, Z. Li, Z.Q. Xiao, F. Yang, D.J. Li, M.Y. Li, F. Li, Z.C. Chen, Triosephosphate isomerase and peroxiredoxin 6, two novel serum markers for human lung squamous cell carcinoma, Cancer Sci. 100 (2009) 2396–2401.

[55] M. Demasi, K.J. Davies, Proteasome inhibitors induce intracellular protein aggregation and cell death by an oxygen-dependent mechanism, FEBS Lett. 542 (2003) 89–94.

[56] Y.H. Ling, L. Liebes, Y. Zou, R. Perez-Soler, Reactive oxygen species generation and mitochondrial dysfunction in the apoptotic response to Bortezomib, a novel proteasome inhibitor, in human H460 non-small cell lung cancer cells, J. Biol. Chem. 278 (2003) 33714–33723.

[57] J. Chandra, Oxidative stress by targeted agents promotes cytotoxicity in hematologic malignancies, Antioxid. Redox Signal. 11 (2009) 1123–1137.

[58] M.V. Sofroniew, Molecular dissection of reactive astrogliosis and glial scar formation, Trends Neurosci. 32 (2009) 638–647.

[59] F. Antunes, E. Cadenas, Estimation of H_2O_2 gradients across biomembranes, FEBS Lett. 475 (2000) 121–126.

[60] S.M. Paine, G. Anderson, K. Bedford, K. Lawler, R.J. Mayer, J. Lowe, L. Bedford, Pale body-like inclusion formation and neurodegeneration following depletion of 26S proteasomes in mouse brain neurones are independent of alpha-synuclein, PLoS One 8 (2013) e54711.

[61] A. Federico, E. Cardaioli, P. Da Pozzo, P. Formichi, G.N. Gallus, E. Radi, Mitochondria, oxidative stress and neurodegeneration, J. Neurol. Sci. 322 (2012) 254–262.

[62] A. Fribley, Q. Zeng, C.Y. Wang, Proteasome inhibitor PS-341 induces apoptosis through induction of endoplasmic reticulum stress-reactive oxygen species in head and neck squamous cell carcinoma cells, Mol. Cell. Biol. 24 (2004) 9695–9704.

[63] M.S. Choy, M.J. Chen, J. Manikandan, Z.F. Peng, A.M. Jenner, A.J. Melendez, N.S. Cheung, Up-regulation of endoplasmic reticulum stress-related genes during the early phase of treatment of cultured cortical neurons by the proteasomal inhibitor lactacystin, J. Cell. Physiol. 226 (2011) 494–510.

[64] R. Xiong, D. Siegel, D. Ross, The activation sequence of cellular protein handling systems after proteasomal inhibition in dopaminergic cells, Chem. Biol. Interact. 204 (2013) 116–124.

[65] E. Ferreiro, I. Baldeiras, I.L. Ferreira, R.O. Costa, A.C. Rego, C.F. Pereira, C.R. Oliveira, Mitochondrial- and endoplasmic reticulum-associated oxidative stress in Alzheimer's disease: from pathogenesis to biomarkers, Int. J. Cell Biol. (2012), (735206).

[66] J.F. Abisambra, U.K. Jinwal, L.J. Blair, J.C. O'Leary III, Q. Li, S. Brady, L. Wang, C.E. Guidi, B. Zhang, B.A. Nordhues, M. Cockman, A. Suntharalingham, P. Li, Y. Jin, C.A. Atkins, C.A. Dickey, Tau accumulation activates the unfolded protein response by impairing endoplasmic reticulum-associated degradation, J. Neurosci. 33 (2013) 9498–9507.

[67] B. Bhandary, A. Marahatta, H.R. Kim, H.J. Chae, An involvement of oxidative stress in endoplasmic reticulum stress and its associated diseases, Int. J. Mol. Sci. 14 (2013) 434–456.

[68] T. Omura, M. Kaneko, Y. Okuma, K. Matsubara, Y. Nomura, Endoplasmic reticulum stress and Parkinson's disease: the role of HRD1 in averting apoptosis in neurodegenerative disease, Oxid. Med. Cell. Longev. (2013), (239854).

[69] J.D. Malhotra, H. Miao, K. Zhang, A. Wolfson, S. Pennathur, S.W. Pipe, R.J. Kaufman, Antioxidants reduce endoplasmic reticulum stress and improve protein secretion, PNAS 105 (2008) 18525–18530.

[70] A. Samali, U. Fitzgerald, S. Deegan, S. Gupta, Methods for monitoring endoplasmic reticulum stress and the unfolded protein response, Int. J. Cell Biol. (2010), (830307).

[71] A.M. Pickering, K.J. Davies, Degradation of damaged proteins: the main function of the 20S proteasome, Prog. Mol. Biol. Transl. Sci. 109 (2012) 227–248.

[72] A.M. Pickering, A.L. Koop, C.Y. Teoh, G. Ermak, T. Grune, K.J. Davies, The immunoproteasome, the 20S proteasome and the PA28alphabeta proteasome regulator are oxidative-stress-adaptive proteolytic complexes, Biochem. J. 432 (2010) 585–594.

[73] T. Grune, B. Catalgol, A. Licht, G. Ermak, A.M. Pickering, J.K. Ngo, K.J. Davies, HSP70 mediates dissociation and reassociation of the 26S proteasome during adaptation to oxidative stress, Free Radic. Biol. Med. 51 (2011) 1355–1364.

[74] Q. Ding, E. Dimayuga, J.N. Keller, Proteasome regulation of oxidative stress in aging and age-related diseases of the CNS, Antioxid. Redox Signal. 8 (2006) 163–172.

[75] X. Wang, J. Yen, P. Kaiser, L. Huang, Regulation of the 26S proteasome complex during oxidative stress, Sci. Signal. 3 (2010) ra88.

[76] R. Shringarpure, T. Grune, J. Mehlhase, K.J. Davies, Ubiquitin conjugation is not required for the degradation of oxidized proteins by proteasome, J. Biol. Chem. 278 (2003) 311–318.

[77] M. Kastle, S. Reeg, A. Rogowska-Wrzesinska, T. Grune, Chaperones, but not oxidized proteins, are ubiquitinated after oxidative stress, Free Radic. Biol. Med. 53 (2012) 1468–1477.

[78] S.A. Hussong, R.J. Kapphahn, S.L. Phillips, M. Maldonado, D.A. Ferrington, Immunoproteasome deficiency alters retinal proteasome's response to stress, J. Neurochem. 113 (2010) 1481–1490.

[79] N.S. Tannu, S.E. Hemby, Two-dimensional fluorescence difference gel electrophoresis for comparative proteomics profiling, Nat. Protoc. 1 (2006) 1732–1742.

[80] T. Rabilloud, M. Chevallet, S. Luche, C. Lelong, Two-dimensional gel electrophoresis in proteomics: past, present and future, J. Proteomics 73 (2010) 2064–2077.

[81] S. Beranova-Giorgianni, Proteome analysis by two-dimensional gel electrophoresis and mass spectrometry: strengths and limitations, TrAC Trends Anal. Chem. 22 (2003) 273–281.